Rock Mech. Rock Engng. (2004) 37 (2), 151–168
DOI 10.1007/s00603-003-0016-x

Rock Mechanics and Rock Engineering
Printed in Austria

Numerical Model for the Analysis of the Evolution Mechanisms of the Grossgufer Rock Slide

By

A. Segalini and **G. P. Giani**

Department of Civil, Environmental and Hydraulic Engineering and Architecture, University of Parma, Italy

Received November 13, 2002; accepted July 16, 2003
Published online November 6, 2003 © Springer-Verlag 2003

Summary

The objective of this paper is to develop a predictive numerical model able to provide indications regarding the triggering of future rock falls on the Grossgufer slope. The work involves the analysis of a previous rock fall event which occurred on the Grossgufer slope during the spring of 1991. This rockslide involved an estimated volume of 30 million cubic meters of rocks and debris. Geomechanical studies and control measurements carried out by the Centre de Researche Scientifique et Applique du Sion (CRSFA) allowed the authors to set up a numerical model able to simulate the rock slope mechanic and hydraulic behavior, and correlate it to the triggering causes of the phenomenon, thus determining a warning threshold for future landslide events.

Keywords: Rockslide, monitoring, numerical modelling.

1. Introduction

The protection of inhabited areas and transportation networks from rock slope instability phenomena involving tens of millions of cubic meters of rocks and debris is, in most cases, impracticable. Because of the dimensions of the potentially unstable rock masses, the associated high volume forces and the complexity of the hydro-geological fields, the placement of efficient active and/or passive measures is almost impossible. Protection of the territory can mainly be limited to safeguarding human lives only by monitoring rock movements and piezometric levels.

The primary problem to be solved then becomes the need to associate the limiting condition for the most probable triggering factor to predefined values of displacements or levels of the groundwater table, hence to a warning system that will signal, sufficiently in advance, the need to evacuate the inhabited areas or close the roadways that

may be destroyed by the expected rockslide. In this regard, it becomes extremely important to know both the amount of hydraulic pressures able to trigger the reactivation of the instability and the phenomenon's evolution mechanics.

This paper will describe the case of the Randa rockslide (Vispa valley, Vallese Canton, Switzerland) where, following a major rock fall, instrumentation for the monitoring and surveillance of the slope was installed.

The Randa rockslide developed during the spring of 1991, as explained by Rouiller (1991, 1992), and can be viewed as one of the most important rockslides of the century: the entire volume of rock, which fell in three different phases (18 and 23 April, and 9 May), was estimated as equal to 30 million cubic meters. Because of the rock falls all roadways were closed, thus interrupting all communications with the high portion of the valley, and the railway and some buildings located on the northern side of the village of Randa were also affected.

The fallen materials formed a natural dam for the River Vispa, originating a lake which, due to the meteorological conditions which led to the snow rapidly melting, soon became a hydrological threat for the entire valley downstream.

Following the first rockslide on April 18, the Department des Travaux Pubblics du Canton du Valais di Sion decided to set up a warning system which was repositioned after each of the two following reactivations.

This work aims at defining the mechanics of the rock fall events by means of a numerical back analysis of the phenomenon, which in turn would allow for the choice of an ''alarm threshold'' to be defined in terms of relative displacements measured within the rock mass, beyond which the development of new rock fall events is more than likely to occur.

2. The Randa Rockslide

2.1 The Event

On April 18, 1991 at 6:20 a.m., an enormous rock fall took place in an area on the left-hand side of the Vispa valley, on the ''Grossgufer'' massif in close proximity to the village of Randa. On April 23 and May 9, two new rock fall events occurred in the same area. The total volume of fallen rock was estimated as 30 million cubic meters and such event is considered the second most important rock fall of the century for the central – western Alpine arc, only preceded by the M.te Zandila (Valtellina, Italy) rock fall in 1987.

The first phase of the rock fall caused a seismic event of 3rd Richter degree magnitude; the fallen material created a dam of the River Vispa, causing the partial inundation of the Randa village and of a few hundred meters of the railway connecting Briga and Zermatt.

Figure 1 shows the slope overlooking the village of Randa and was taken shortly after the last rock fall event. Figure 2 displays the central vertical section that was the seat of the movement. Precisely, Fig. 2 shows the orientation of discontinuities (on the cross section) that separated the rock volumes then involved in the rock fall.

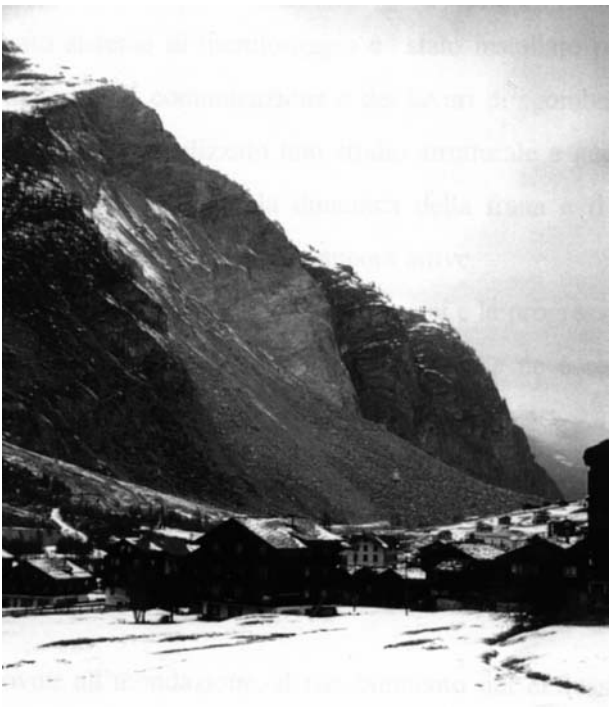

Fig. 1. The Randa rock slide as viewed from the opposite side of the valley and downstream. The picture was taken shortly after the last rock fall event

The data reported relating to the geological studies and on-site control measurements were kindly provided by the former CRSFA, Centre de Researche Scientifique et Applique du Sion (Rouiller, 1991, 1992; Wagner, 1991; Schindler, 1995).

The sliding slope belongs to a rock mass which is part of the Siviez-Mischabel fault and is characterized by a monotonous series of paragneiss and ortogneiss (gneiss of Randa), as described by Sartori (1991). The contact between the two rock formations dips at 20°–30° inside the slope. The schistosity of the formation also dips at 20°–40° inside the slope.

2.2 Control Measurements

The control instruments were in place before the event of April 18. Such instrumentation was replaced each of the three times that the rock fall took place. The control system is formed by a geodetic network coupled with extensometer stations, and a seismic surveying network. The geodetic network consists of a series of reflectors distributed on the crown of the main scarp and is used for general control. The extensometer network is dedicated to monitoring the relative displacements of different discontinuities, mainly the variation of their aperture, and its purpose is provide information for post-alarm control.

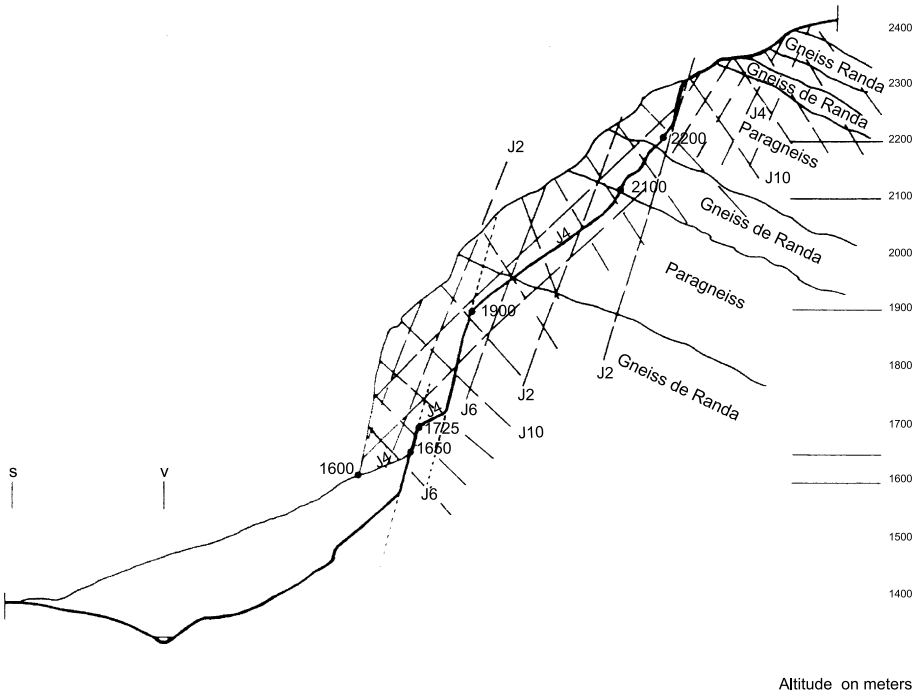

Fig. 2. Standard section of the area of the Grossgufer massif that was involved in the rockfall phenomenon. The bold line indicates the slope profile after the event. (from Rouiller, 1992)

Figure 3 shows some of the results of the extensometer monitoring carried out in the time span between April 28 (five days after the second rock fall event) and May 9, when the last rock fall took place. The reported curves refer to extensometers located inside several tension cracks which, in terms of orientation and spacing, belong to discontinuity set J2 or J6. A geometrical model of the rock mass forming the slope was generated with the purpose of reconstructing the geomechanical behavior of the monitored discontinuities.

The seismic control network was developed with the purpose of determining, on the basis of the registered seismic activity, an alarm threshold for the evacuation of the population of Randa.

Immediately after the last rockslide, a weather station was set up, together with other climatic instruments, in order to work out any possible correlation between measured displacements and actual climatic conditions. The instrument readings were automatically recorded and radio transmitted on a daily basis from the central station, located on top of the Grossgufer massif, to a remote control center at the bottom of the valley; should a critical situation arise, the frequency of transmissions can be increased interactively from the remote control center.

During the first few days after the last rock fall, when workers were deployed to restore the accessibility of road and railroad connections, and drain the basin that had formed upstream of the rock fall deposit, a network of observers equipped with radio

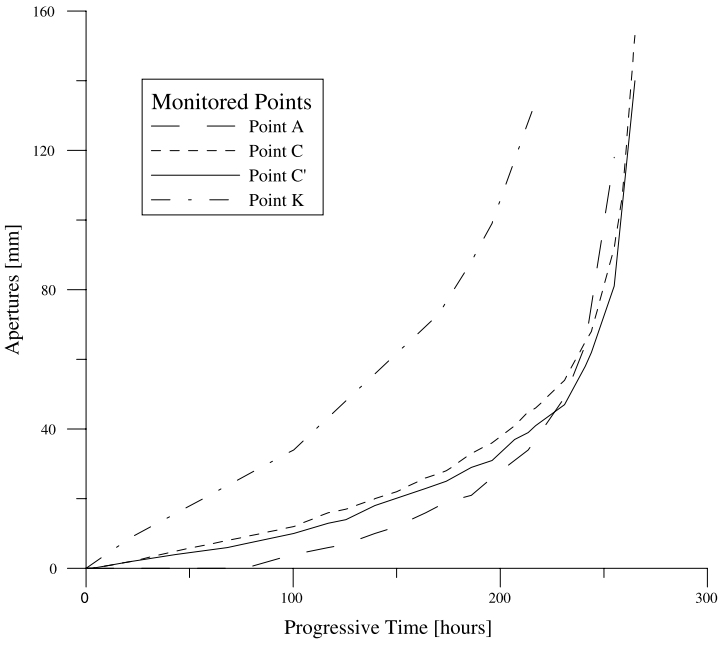

Fig. 3. Extensometer measurement taken between April 28th and May 5th, 1991. The reported diagrams are referring to extensometer located in close proximity of the points monitored in the numerical model (see Fig. 5)

transmitters were deployed to signal any danger imposed by a possible detachment of individual blocks.

3. Structural and Geomechanical Study

The geomechanical study was carried out by means of on-site surveying performed at different measurement stations, mostly located at the top end of the Randa gneiss outcrops, in close proximity to the main detachment scarp.

The measurement stations that were destroyed by the second and third rockslide event were replaced with other new locations set out in close proximity to the current main scarp and, since then, have been giving results that are substantially consistent with those recorded after the first rockslide event.

The structural analysis was carried out for the former CRSFA by Wagner (1991) and was based on an extensive geomechanical survey; it allowed the identification of four main discontinuity sets, which are recurrent within the Grossgufer massif (J4, J10, J2 and J6).

The data are reported in Fig. 4 using a spherical projection, as curves of equal frequency of the discontinuity plane poles. Sets J2 and J6 are sub-parallel, dipping outside the slope with a dip angle higher than the one of the slope. Set J10 dips inside the slope, with dip angle similar to those of sets J2 and J6 (Fig. 2).

The potential kinematic mechanism of instability found in the area of interest for the study on the Grossgufer massif is due to the presence of discontinuity set J4 which, dipping outside the slope with a dip angle slightly lower than the slope angle, is

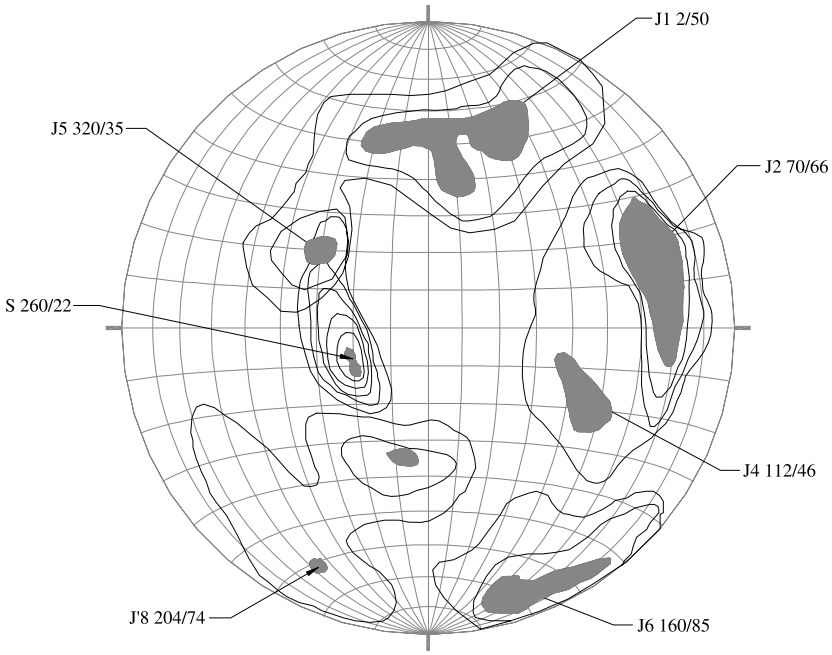

Fig. 4. Stereographic representation of the most significant joint sets mapped on the Grossgufer massif

responsible for the formation of a sliding plane. Such a geometrical feature is recognizable from the slope geometry after the rock fall phenomenon, where the formation of a stepped surface was observed on the summit of the slope, i.e. where J2 and J6 discontinuity sets originate the rise, and set J4 forms the tread.

In addition to the key role played by discontinuity set J4 for the structural control of the rock mass, the secondary role of the three other discontinuity sets must be mentioned. Because of their dip angle characteristics, these sets contribute to the strongly anisotropic secondary permeability, which favors the percolation of water until it reaches discontinuity set J4 deep inside the rock mass.

The average geomechanical features of the discontinuity sets, considered as the most relevant for the stability analysis of the slope, are as follows:

– set J4: spacing = 3 m, aperture = 12 cm;
– set J2: spacing = 3.7 m, aperture = 12 cm;
– set J6: spacing = 3 m, aperture = 1 mm.

4. Causes of the Rock Fall Phenomenon

The causes of the rock fall phenomenon can be divided into two categories: originating and instigating. Among the originating causes are those of tectonic origin, connected with the genesis and subsequent weathering of the metamorphic rock mass, and with the tectonic displacement that developed in conjunction with the numerous faults dislocated in the surroundings of the area of interest (Wagner, 1991), and those of

climatic nature, induced by the latest glaciations the rock mass was subjected to. Among the instigating causes of the phenomenon, apart from any seismic activity which can be ruled out considering the monitoring system outcome, a primary role was played by the rise in the water table, as described by Schindler (1995); this rise was induced by the snow accumulation recorded in the highest part of the basin and is associated with the increase in temperature and the rain precipitation recorded in the fortnight just before the rock fall event.

5. Numerical Modeling of the Phenomenon

The aim of this study, as already mentioned in the introduction, is to develop a predictive numerical model able to provide indications regarding the triggering of future rock falls on the Grossgufer slope.

In order to develop a reliable numerical model dependable geometrical and mechanical features are necessary. It is impossible to acquire all the parameters needed for the numerical simulation from the surface survey, particularly for those governing the behavior of the rock mass in depth, so the model was calibrated using a back analysis procedure, based on the data registered before the rock fall events.

The back analysis was carried out in order to obtain consistency between the displacements calculated from the numerical results and those measured during the monitoring of discontinuities.

In order to choose the most suitable numerical modeling method and formulate a suitable solution for the alarm threshold definition, several preliminary thoughts are needed.

The limit equilibrium method (LEM) did not appear to be appropriate for a few basic reasons, among which is the impossibility of taking into account the joint stiffness, the deformation modulus of the rock blocks, the crack propagation phenomenon and the progressive failure of the slope, as stated by Giani (1992). In addition, the limit equilibrium method does not take into account the influence of the state of stress evolution over the equilibrium conditions of the potentially unstable rock masses. Some numerical methods allow to overcome, completely or partially, the limitations imposed by the limit equilibrium method. Nowadays, the methods most commonly used in rock mechanics are: the finite element method (FEM), the distinct element method (DEM) and the boundary element method (BEM) (Barla and Barla, 2000).

The finite element method allows a detailed modeling of the rock mass state of stress, of the different deformations of rock and soil, of the constitutive laws for the geological media and of the main faults and discontinuity sets. This method is limited because it considers only a small deformation field, the discontinuities must be modeled as completely persistent (substantial impossibility of simulating crack propagation), the possibility of carrying out stability analysis in the static field is limited, and the proximity to the instability phenomenon can only be considered through the examination of shear and tension zones within the model.

The distinct element method allows to model the slope as a system of blocks (both rigid and deformable), and also model the various phases of the rock mass genesis, record the displacements of single blocks (relative or total) and analyze the associated behavior of continuous and discontinuous media when coupled with the boundary

element method (Cundall, 2001). With the above in mind, the use of the distinct element method appeared to be the most suitable.

Another problem to be addressed was the choice of the dimensional space in which the numerical modeling would be carried out. Although a digital terrain model of the slope was available, a three-dimensional distinct element model was regarded as being too susceptible to the variation of the high number of parameters involved in the definition of the mechanical characteristics of the joints, many of which were not known directly and obtainable from technical literature only.

In order to find the most significant section of the rock mass in terms of critical conditions for the stability of the slope, the massif was analyzed as a whole using the key block theory, developed by Goodman and Shi (1985), which allowed the definition of removable blocks having 4, 5, 6 and 8 faces.

The key block theory is based on finding rock blocks completely separated from the rock mass by discontinuities, defined as critical because once they are detached from the rock mass they free other blocks and trigger a larger rock fall phenomenon. The method can be used, in the case of a rockslide study, for a preliminary structural

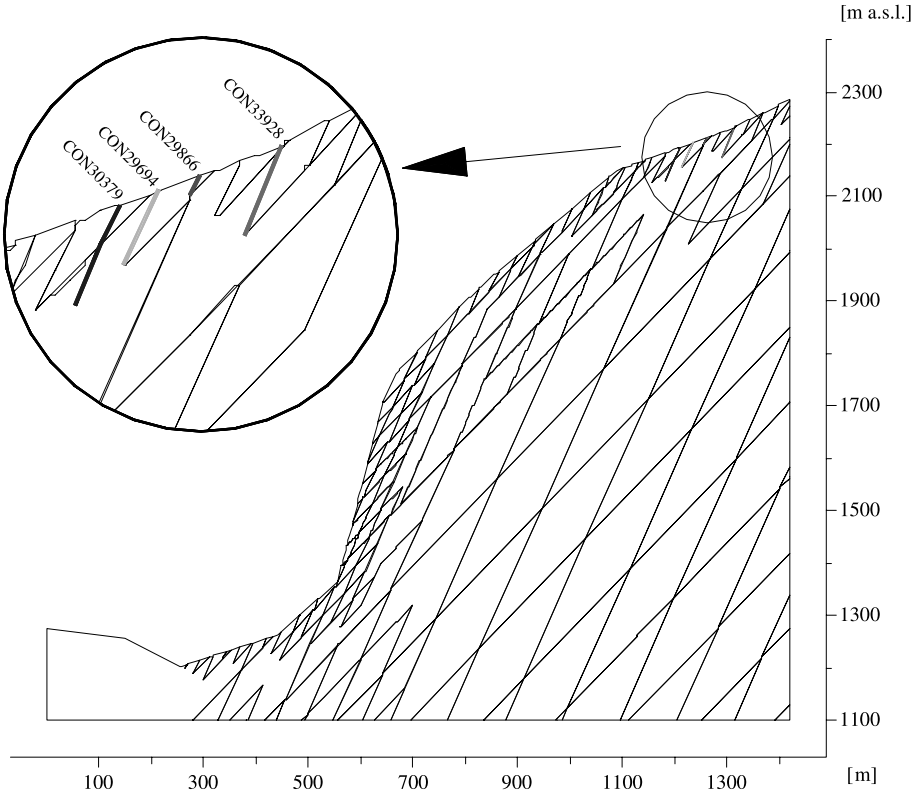

Fig. 5. Section used for the 2-dimensional distinct element analysis (UDEC), with the indication of the contacts subjected to extensometer monitoring

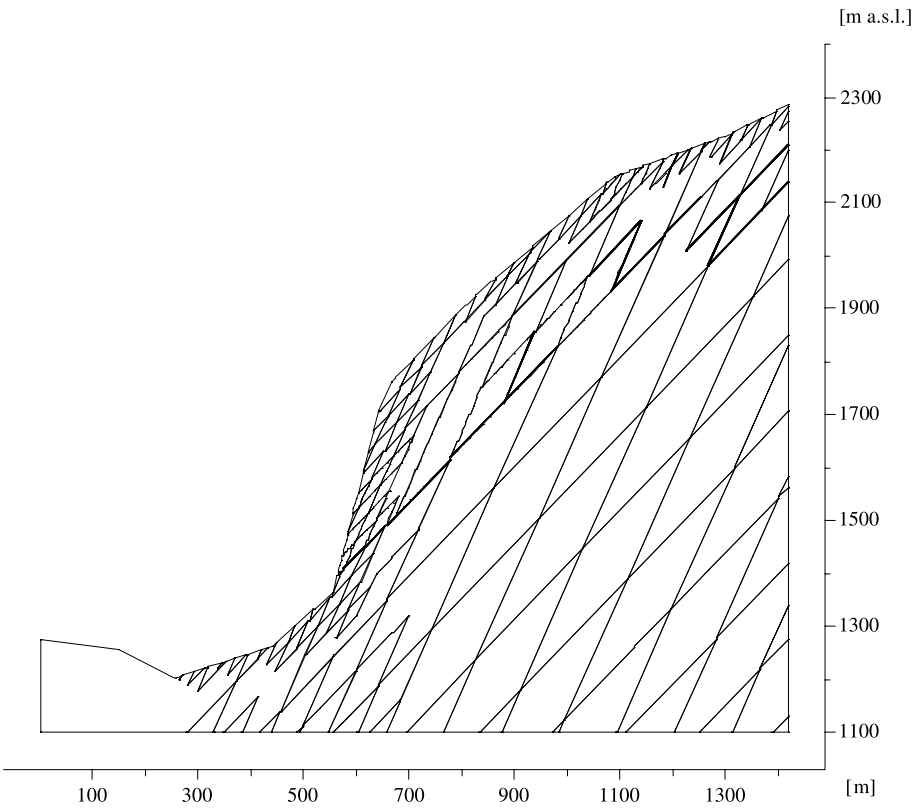

Fig. 6. Shear displacements on joints as calculated from 2-dimensional distinct element analysis (UDEC); the thickness of the lines corresponds to the amount of occurred shear displacement. It can be noticed how the model returns a good indication of the stepped surface of rupture that has been observed after the rockfall

analysis aimed at the recognition of the unstable areas and of the likely kinematic mechanisms to be expected on the slope.

The methodology assumes that the discontinuity surfaces are perfectly planar and persistent and the blocks not deformable. The mathematical theory on which the method is based is expressed in geometrical and topological terms, while the stability conditions are examined in static terms.

The objective of the analysis carried out on the Randa slope is to highlight the presence of removable blocks and their preferential direction of movement.

The vertical section chosen for the numerical analysis is the most critical one, according to the methodology proposed by Goodman and Shi (1985), and identifies the prominent role of discontinuity set J4 (46,110) for the overall stability of the rock slope.

The frequency of the kinematic mechanisms in which set J4 plays a predominant role is much higher than any other mechanism developing along intersection lines J4–J2 and J4–J6.

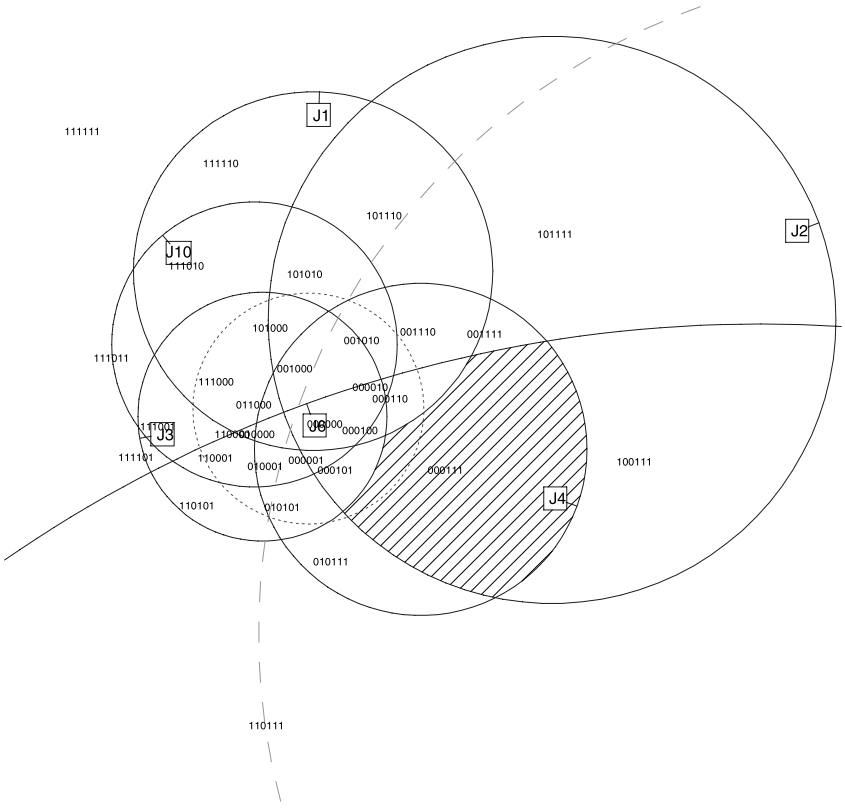

Fig. 7. Joint pyramid obtained from the analysis carried out with the key block theory (Goodman and Shi, 1985)

The most significant results obtained from the key block stability analysis are summarized in Figs. 7 and 8. Reported in Fig. 7, using the stratigraphic projection, are the mean circles of discontinuity sets J1, J2, J3, J4, J6 and J10, and highlighted are the joint pyramids composed between the various planes.

From the data obtained with the discontinuity survey, particularly for joint aperture, roughness and persistence, it appears obvious that the friction angle values are not adequate to guarantee the block stability, particularly when high hydraulic pressures are developing as a consequence of the rise in the water table.

The numerical modeling was then carried out on the most significant section of the Grossgufer massif, where the discontinuity sets pointed out by the geomechanical analysis were producing the most significant effect for the stability condition of the slope.

The condition examined is, undoubtedly, the most critical one if compared with any other three dimensional numerical model of the slope. Since the numerical modeling is aimed at the definition of a risk threshold for any possible future rock fall, the above choice appeared to be appropriate, considering both the lower subjectivity for the parameter definition and the support of the preliminary three dimensional analysis of the possible kinematic mechanisms carried out by means of the key block theory.

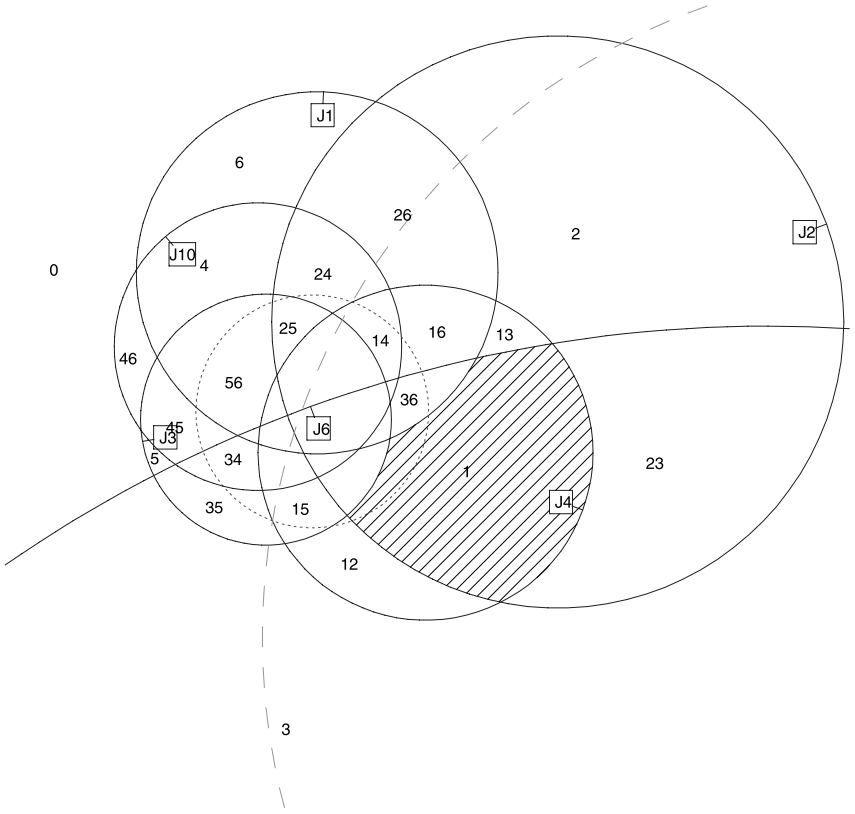

Fig. 8. Equilibrium region obtained from the analysis carried out with the key block theory (Goodman and Shi, 1985)

The distinct element code, developed by Cundall (1980), remains the most suitable for the numerical modeling of fractured rock masses, particularly when the discontinuity sets are fully persistent, as observed in the Grossgufer massif. This code allows to define the presence of water within the joints and, consequently study the effects induced by the water flow inside the discontinuities.

The distinct element model was built using deformable elements in its upper portion, where the slope is reproduced, and rigid blocks in the lower portion. This was done in order to ease the calculation phase and allow the application of appropriate boundary conditions.

The numerical modeling consists of two phases. The first is aimed at the reconstruction of the original stress and strain configuration within the rock slope as expected in the morphological situation preceding the last rock fall event. This was done considering the morphological situation as topographically surveyed and with the hypothesis of complete drainage of the rock mass. The second phase determines the stress and strain state within the rock mass associated with the progressive rise in the water table.

The water table level increments were applied as a variation of hydrostatic conditions at the inner boundary of the model. The calculation, once the new hydraulic boundary condition is set, develops towards the steady state condition using fully coupled criteria. The variation of hydraulic pressure within the discontinuities generates a variation of joint apertures and, therefore, a relative displacement between the blocks surrounding them.

The modeling of the second phase of the rock fall phenomenon was carried out by means of a back analysis of the last events, in order to find a critical hydraulic threshold that, once reached, does not allow the readjustment of the state of stress within the rock mass, so that the stability of the slope evolves independently and irreversibly towards failure.

5.1 Geometry Definition

As mentioned above, of the several sections available for the massif, the choice was directed towards the one shown in Fig. 5, which represents the most critical stability situation. Specific attention was devoted to the choice of a section where the extensometer measurements, coming from the tension cracks monitored behind the rock slide crown, could easily be reported and, consequently, compared with the numerical results. The reconstruction of the joint pattern of the rock mass was carried out following the indications obtained from the structural survey and the considerations regarding the significance of the various joint sets.

In order to define the hydraulic pressure which is critical for the overall stability of the slope, the position of the ground water table was progressively raised inside the Grossgufer massif during DEM modeling.

The vertical section of the slope considered extends from the altitude of 1,400 m a.s.l, corresponding to the River Vispa, to the altitude of 2,400 m a.s.l, where the most remote instruments for the measurement of the discontinuity aperture were installed, and their data is recorded and available for comparison (Fig. 5).

The surface of the slope was the most intensely fractured, as demonstrated after the rock fall when new outcrops were observed and compared with the surfaces originally surveyed. The intense fracturing observed on the rock surfaces appears to be ascribable to both the effects of the decrease in the stresses due to the glacier retreat, and the progressive weathering of the exposed surfaces.

5.2 Material Properties and Constitutive Laws

In order to carry out a stress-strain analysis it is necessary, first of all, to assign the mechanical properties and the constitutive laws that are most appropriate for the rock matrix and the joint sets.

The mechanical features of the rock matrix, with particular attention to the deformation modulus and the compressive strength, were known from the studies carried out by the Centre de Researche Scientifique et Applique du Sion (Rouiller, 1991, 1992; Wagner, 1991; Schindler, 1995).

During the numerical calculation, the model assumes that the discontinuities are either completely persistent or unable to propagate, so that no block could contain

Table 1. Mechanical characteristics assigned to geomaterials and discontinuities within the numerical model

	Mechanical properties of materials						
	γ [kg/m^3]	K [Pa]	G [Pa]	c [Pa]	ϕ [°]	τ [Pa]	
Rock matrix	2600	1.66E + 10	7.60E + 09	5.00E + 05	38	1.00E + 08	
	Orientation [°]	jkn [Pa/m]	jks [Pa/m]	jc [Pa]	jϕ [°]	jτ [Pa]	jdil [°]
J4 joint set	46/112	8.00E + 06	4.00E + 06	3.00E + 05	28	1.00E + 04	10
J2 joint set	66/70	8.00E + 06	4.00E + 06	3.00E + 05	32	1.00E + 04	10

isolated discontinuity portions; therefore the following values were assumed for the model:

- density $\gamma = 2{,}600\,\text{kg/m}^3$;
- bulk modulus $\text{K} = 16.6\,\text{GPa}$;
- shear modulus $\text{G} = 7.6\,\text{GPa}$;
- cohesion $\text{c} = 0.5\,\text{MPa}$;
- friction angle $\phi = 38°$.

The constitutive law was chosen as elastic perfectly plastic with the Mohr-Coulomb yield surface. Considering the joint sets, the mechanical properties of each set could be identified, considering both the set membership and weathering. The mechanical features associated with the joint sets are reported in Table 1.

The constitutive laws for the joints are elastic perfectly plastic according to the Coulomb criterion. The discontinuity walls appear to be weathered by the presence of water flow, which with the increase in internal pressure, determined the washing away of the fine filling that was previously observed in most of the joints. Such action appears to be most intense along joint set J4 (46°/110°) where the lower dipping angle allowed the most intense filling deposition under ordinary water pressure regime.

The discontinuity sets exhibit the following orientations:

- discontinuity set J4 dips outside the slope with an average angle of 46°;
- discontinuity set J2 dips with an angle of 66°, higher than the average angle of the slope face.

The residual friction angle of these sets is influenced by weathering of the walls, while the dilation angle is governed by the low state of stress on these walls due to their limited depth and is therefore assumed equal to 10°. The joint normal (jkn) and shear (jks) stiffnesses were assumed to be homogeneous for the two sets, considering both the homogeneity of the rock mass and the joint shear behavior.

5.3 Boundary Conditions

The numerical model was fixed at the base, in order to prevent vertical displacements, and at both sides to prevent any horizontal displacement of the boundaries. The size of

the model was estimated to minimize the boundary effect in the area object of study, i.e. where the instability phenomenon is developing. This kind of choice is always necessary in order to obtain a good compromise between calculation economy and reliability of the results.

5.4 Analysis Procedure

The distinct element analysis was carried out in several steps.

The first step, named consolidation, was performed in order to reconstruct the original state of stress in the slope, as it was before the rock falls.

The following steps were then carried out in order to study the coupled flow – deformation problem versus time, just after heavy rainfall or rapid snow melting events, when the water table level rises inside the discontinuities.

The first step was accomplished by introducing the specific weight of the single elements in the model. The geometry of the slope was equivalent to the one measured on-site before the last rock fall event. The state of stress induced by the gravity forces was assumed as the initial state of stress. The absolute displacements derived from the application of the gravity forces on the slope were zeroed.

Five calculation steps were carried out to simulate heavy rainfall and/or infiltration of water due to snow melting and the subsequent rise in the water table. Associated to each step was a water table rise of 200 m, starting from an altitude of 1,100 m a.s.l., representing a completely drained slope, and ending at the maximum altitude reached by the water table at 2,100 m a.s.l.

During these calculation steps the analysis can be assumed to be coupled since the aperture of the discontinuities varies in relation to the hydraulic pressure reached inside the joints. As a consequence, the conductivity of the discontinuities increases with the joint aperture and decreases with their closure. The presence of hydraulic pressures inside the joints lowers the effective normal stresses and, consequently, the shear strength that can be mobilized.

As previously said, the discontinuities in the model were assigned shear resistance, normal and tangential stiffness, and aperture (see Table 1) according to their joint set membership and consistently with what was measured during the on-site survey.

These properties vary with the water table height and with the reciprocal displacement of adjacent blocks. In particular, while the aperture of the discontinuities increases with the rise in the water table and the normal stiffness decreases, the slipping between blocks causes the reduction in shear strength and shear stiffness.

5.5 Numerical Modeling Results

The results of the numerical modeling can be analyzed by examining the trends of the normal and shear stresses, hydraulic pressure on the joint faces, and the relative and absolute displacements of the blocks.

The ratio between the mobilized shear strength and the calculated shear strength provides, for each joint within the model, the sliding safety factor of the block resting on a given joint.

If, for each of the five calculation steps where the water table rises, one examines the results in terms of local safety factors of the blocks, it can be noticed that there are no significant detachments of blocks from the slope, neither for sliding nor toppling, before the water table reaches an altitude of 1,800 m a.s.l. When the water table reaches 1,850 m a.s.l altitude, limit equilibrium surfaces formed by several adjacent joint interfaces begin to develop. In particular, the unstable blocks are located on the lower section of the sub vertical cliff forming the slope, beginning at the altitude of 1,440 m a.s.l.

The progressive rise in the water table increases the number of interfaces where the maximum strength available is reached. This continues until the water table reaches 2,100 m a.s.l, when a complete failure surface, formed by the joints sets J4 and J2, develops, similar to the one estimated following the last failure event (Fig. 6).

Figure 9 shows the aperture displacement trend induced by the rise in the water table within the model. As reported in the previous paragraph, the generation of the numerical model was carried out so as to obtain the highest possible agreement

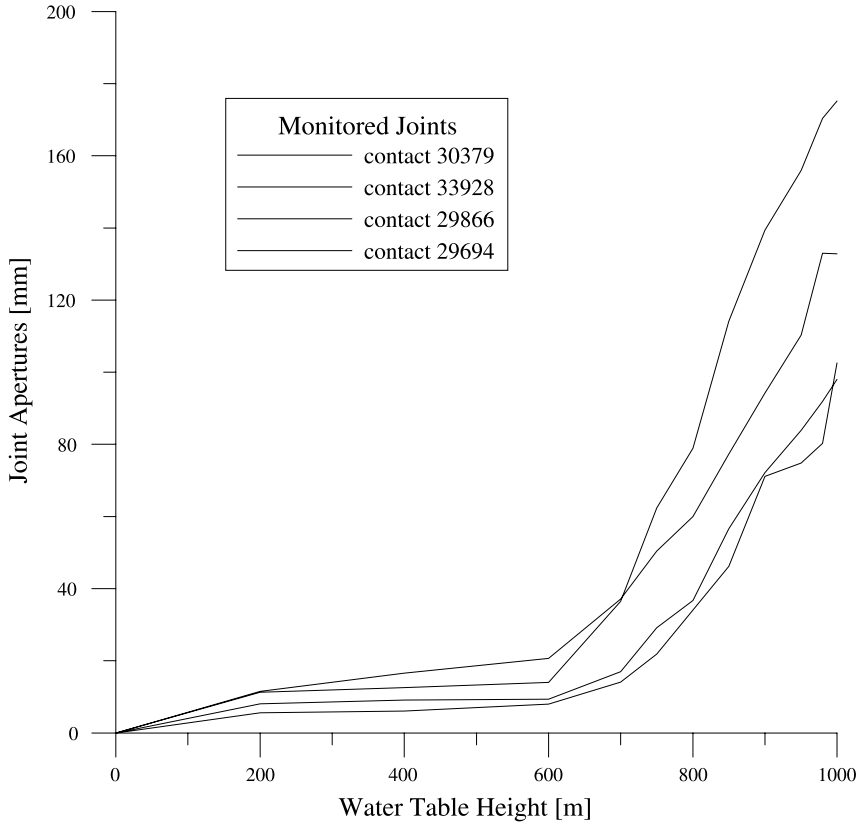

Fig. 9. Joint aperture trend calculated from the numerical model of Fig. 5. The reported curves are comparable with those obtained from the extensometer monitoring

between the real geometrical position of the monitored joints and the position they have in the numerical model.

Figure 9 shows the joint aperture trend with the rise in the water table. The increment in the aperture is linear until the water table reaches 1,700 m a.s.l. altitude, becoming then quadratic for further increments in the water table altitude and reaching a clear condition of instability for levels higher than 2,000 m a.s.l.

It can be noticed that, before reaching 1,700 m a.s.l. altitude of the water table, the aperture increments are contained between 10 and 20 mm, while for levels of the water table above 2,000 m a.s.l. altitude, they vary between 80 and 150 cm. Therefore, the alarm threshold can be considered as the one that corresponds to the beginning of the non-linearity of the diagram aperture-water table level, corresponding approximately to 1,700 m a.s.l. altitude.

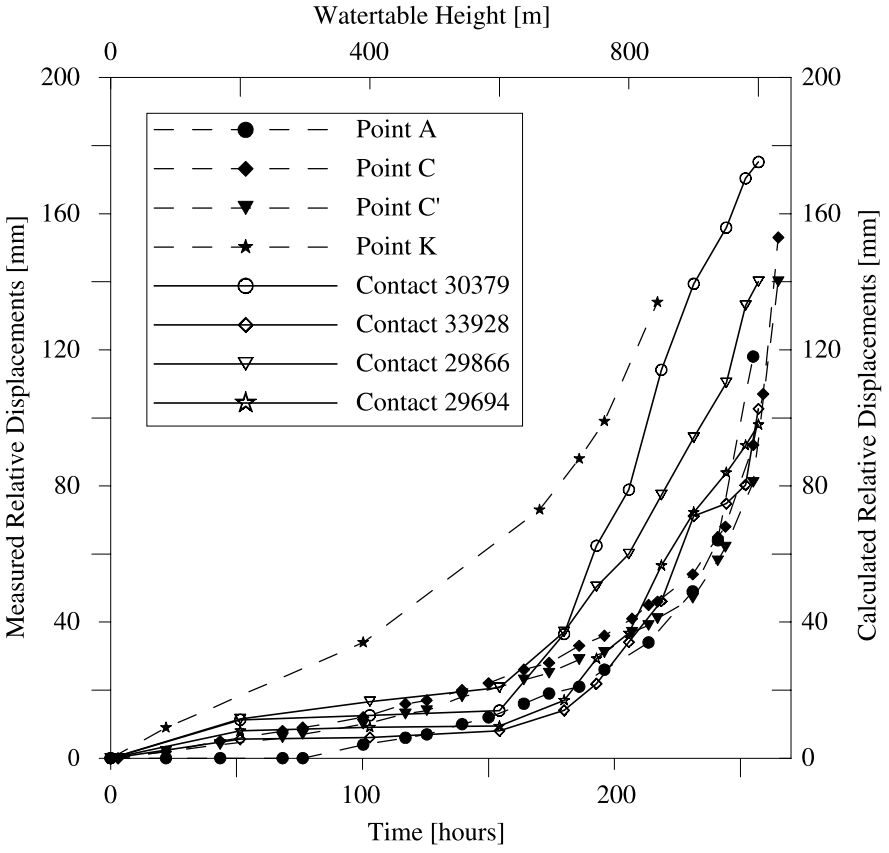

Fig. 10. Cumulative diagram of the joint aperture curves, obtained overlapping the real trend (from the in situ survey) and the numerical results. From the comparison it is clear that the values of the relative displacements of the joints are almost identical between the numerical model and in situ measurement; the similarity time – water table level is obtained as a consequence

5.6 Comparison Between Field Measurements and Numerical Results

The comparison between field measurements of discontinuity apertures and numerical results requires a correlation between time and water table increments.

It is known that the rock fall events that took place in Randa between 18 April and 9 May 1991 were triggered by the infiltration of water in the rock mass due to rainfalls together with the melting of the snow cover. However, the time taken for the infiltration to occur and the levels of water table reached before the event are not known. An attempt at the correlation time – water table increment was made, as illustrated in Fig. 10.

The joint aperture monitoring was carried out for a period of approximately 265 hours (April 28–May 9, 1991), and the best fit between experimental data and numerical results can be obtained considering a linear variation of the water table level in time. The best fit is obtained, in particular, when considering an increment of 400 m in the water table level every 100 hours. This corresponds to an increase in the water table altitude of approximately 100 m per day.

The main contribution to the water infiltration in the rock mass is due to the snow melting, so it is not possible to reconstruct the correlation between the rise in the water table and the precipitation using a hydro-geological balance, even if the amount of rainfall was measured during the days preceding the rock fall.

It must also be noted that, although starting from an arbitrary hypothesis such as the completely drained slope at the time when the first aperture measurement was taken, a very good result in terms of agreement between field measurements and calculated data was reached. It must be noted, in fact, that the most important result is related to the fact that the diagram displacement-time becomes non-linear. This consideration means that, even in the hypothesis of starting the numerical modeling from another arbitrary situation of the water table (i.e. 1,400 m a.s.l), the results in terms of water table level threshold for the uncontrolled development of the rock fall do not change (i.e. 1,700 m a.s.l.).

6. Conclusions

The purpose of this study was the development of a numerical model that, once validated through a comparison between numerical results and field measurements, would be useful to define the hydro-geological flow regime that determines the rock fall triggering threshold.

The development of such a numerical model required the reconstruction of the geometry of the discontinuity distribution along the central cross section of the slope under study, the geomechanical characterization of the rock mass, and the definition of a sequence of hydraulic conditions rising from the bottom of the slope to the level at which the slope collapse occurred.

The validation of the numerical model, carried out through the comparison of the diagrams of the apertures of the modeled joints and those measured on-site, showed a very good agreement between the numerical results and the field measurements. This agreement proved to be good for both the relative displacements recorded along single

discontinuities and the trends of the diagrams reporting relative displacements vs. time and relative displacements vs. water table height.

It should be noted how, in the diagrams derived from field measurements, the relative displacements vs. time curve is characterized by two sectors having different inclinations – sub-horizontal the former and sub-vertical the latter – and separated by an elbow. Likewise, in the diagrams derived from the numerical calculation the curve relative displacements vs. water table height shows two sections separated by an elbow. This elbow, reached at an average value of 40 mm for the aperture of the monitored joints, defines the stability condition threshold for the Grossgufer slope and should therefore be used to define the critical alarm state.

Acknowledgments

The Authors wish to thank Dr. J. D. Rouiller and Dr. C. Marro, of the former CRSFA of Sion, for granting permission to use their data and for their precious help in understanding the geological configuration of the Vispa valley.

References

Barla, G., Barla, M. (2000): Continuum and discontinuum modelling in tunnel engineering. Gallerie e Grandi Opere Sotterranee N. 61, August.

Cundall, P. A. (1980): A generalized Distinct Element Program for modeling jointed rock. Peter Cundall Associates, Report PCAR-1-80; European Research Office, U.S. Army.

Cundall, P. A. (2001): A discontinuous future for numerical modelling in geomechanics? Proc. Institution of Civil Engineering. Geotechn. Engng. 149(1), 41–47.

Giani, G. P. (1992): Rock slope stability analysis. Balkema, Rotterdam, 361.

Goodman, R. E., Shi, G. H. (1985): Block theory and its application to rock engineering. Prentice Hall, London, 338.

Rouiller, J. D. (1991): Bergsturz Grossgufer – La catastrophe de Randa 1991. CRSFA, Centre de Recherches Fondamentales et Appliquees de Sion.

Rouiller, J. D. (1992): Bergsturz Grossgufer/Randa – Eboulement de Randa. Strase Verkehr 5. 373–376.

Sartori, M., Schafer, M., Escher, A. (1991): Rapport concernant un premier stade d'evalutation des causes geologiques de l'ebolument de Randa. Université de Lausanne, Institute de Geologie et Paleontologie.

Scavia, C. (1990): Fracture mechanics approach to stability analysis of rock slopes. Engng. Fract. Mech. 35(4/5), 899–910.

Schindler, C. (1995): Influence de l'eau sur l'eboulement de Randa. CRSFA, Centre de Recherches Fondamentales et Appliquees de Sion.

Wagner, A. (1991): Bergsturz Grossgufer/Randa – Étude structurale et geomecanique. CRSFA, Centre de Recherches Fondamentales et Appliquees de Sion.

Author's address: Dr. Andrea Segalini, Department of Civil, Environmental and Hydraulic Engineering and Architecture, University of Parma, 43 100 Parma, Italy; e-mail: andrea.segalini@unipr.it